Cumhuriyet Science Journal

Efficient Methanol Electro-oxidation on Ni, S Dual Doped Reduced Graphene Layer Catalyst

Rukan Suna Karatekin [1,a,*], Sedef Kaplan [1,b]

[1] Science Faculty, Mersin University, Mersin, Türkiye.
*Corresponding author

Research Article

ABSTRACT

Energy crisis is the most popular issue in the world, which must be overcome with the development of alternative energy sources. Among them, methanol is a promising fuel when used in direct methanol fuel cells. However, the mentioned cell needs highly electroactive and stable anode materials toward MeOH. Ni has gained attention as it is an alternative to noble atoms. In this study, Ni was deposited on reduced graphene layer which functionalized with S atoms via the hydrothermal method. The fabricated sample was characterized by using Scanning Electron Microscopy (SEM), Energy Dispersive X-ray Spectroscopy (EDX), mapping, X-ray Powder Diffraction (XRD), and Brunauer–Emmett–Teller method (BET). Two samples as called Ni/GCE and Ni@s-rGO/GCE were examined for methanol oxidation reaction in alkaline media. For methanol oxidation, due to the higher surface area, and small particle size of Ni, the mass activity of Ni@s-rGO/GCE is two times higher than Ni/GCE

Keywords: Methanol oxidation, s-doped reduced graphene, Ni nanoparticles.

[a] rukansuna@mersin.edu.tr   https://orcid.org/0000-0003-3052-1539   [b] kaplansedef33@gmail.com   https://orcid.org/0000-0002-3345-1452

Introduction

Fuel cells have effective approaches for the conversion of energy due to their high efficiency, low energy consumption, clean, and quick refueling characteristics [1]. Among them, Direct methanol fuel cells (DMFCs) have great attention due to their high energy density, safe storage and transportation, simple operation, and environmental friendliness. Additionally, methanol has a low molecular weight, low cost, high specific energy density, and simplicity of storage [2]. Pt and Pt-group metals have been used as anode materials to improve the methanol oxidation in DMFC. Due to the high cost of these metals and their poisoning property, a new alternative electrode material has been researched.

Nickel is a transition metal that because of its surface oxidation property gain the potential to be used as a catalyst for different electrochemical reaction. It is reported that Ni is an alternative material because it is cheap and abundant, that shows excellent catalytic activity toward methanol oxidation in alkaline media [3]. The oxophilicity of Ni allows the forming OH groups to be active sites at the surface of the catalyst; thereby antipoisoning property of the catalyst increases [4]. For this reason, Ni based catalysts have been used as an alternative to noble metals especially in alkaline medium [5].

It is well known that the catalytic activity of an electrode depends on its morphology, particle size, active surface area, and ability of methanol adsorption. Recently, in some studies, Ni nanoparticles were synthesized on different supporting materials and examined for MOR. For example, Ji et all, deposited Ni on

N-doped carbon frameworks (CFNs) and used this fabricated electrode for MOR. They emphasized that the interactions between Ni and CFNs supported the forming of smaller particle sizes of Ni, and uniform dispersion on CFNs. So, with attended these two effects, the reaction kinetics of methanol oxidation increased [6]. Liu et all., synthesized pure Ni nanocrystalline anchored on rGO and examined it for methanol oxidation reaction (MOR) under alkaline conditions. They reported that due to the synthesis of Ni with ultra-nano size on rGO the active surface area increased and this situation improves the mass activity toward methanol oxidation and antipoisoning property of the catalyst [7].

To obtain uniform and nanosize metal nanoparticles, carbon-based materials have been used commonly. In the last studies, reduced graphene oxide (rGO) has been used as a supporting material for this purpose. Besides, rGO has excellent properties such as conductivity, and higher surface area, when compared to other carbon materials [8, 9]. Furthermore, the properties of rGO such as stability, conductivity, surface area, and catalytic activity enhance with dopant (heteroatoms, anionic or cationic surfactant) loading.

In this study, Ni nanoparticles were synthesized on reduced graphene oxide which functionalized with sodium dodecylbenzene sulfonate (SDBS) via the hydrothermal method. Fabricated Ni@S-rGO electrode was examined for MOR under alkaline conditions. To investigate the supporting material effect on the performance of Ni for MOR, Ni nanoparticles were

synthesized by hydrothermal method without supporting material.

Materials and Methods

S-rGO Synthesis

Firstly, graphene oxide was synthesized by Hummer's method [10]. The other steps were mentioned in our previous study[11] . Briefly, a certain amount of GO was dispersed in 120 mL of bi-distilled water after 1h, and 120 mg SDBS was added to the GO solution for 30 minutes. Then hydrazine solution was added to the homogenous solution and the prepared solution was refluxed for 24 h. This solution is used directly when synthesizing Ni@SrGO.

Ni@S-rGO synthesis

25 mL of as-prepared s-rGO, 118 mg of nickel chloride hexahydrate (NiCl$_2$.6H$_2$O), and 30 mL of ethylene glycol were mixed with a magnetic stirrer. Also, 0.5 g of sodium hydroxide (NaOH) was dissolved in 10 mL of 80% hydrazine (N$_2$H$_4$) in a different beaker. This solution was dropped slowly into other solutions and was mixed for 15 minutes. The prepared solution was transferred into a Teflon-lined autoclave at 200 °C for 1 h. After 1h of waiting the cell cooled down and the sample was centrifuged and washed with water and methanol several times. Finally, it was left to dry in the drying oven.

Characterization and Electrochemical Measurement

The X-ray diffraction spectra were obtained by Empyrean, Panalytical, operated in a 2θ scan from 20° to 90° and with Cu-Kα irradiation as an X-ray source (40 kV/30 mA). Quanta 650 field emission microscopy (FESEM) and energy dispersive X-ray spectroscopy (EDS) were used to identify the morphology and elemental composition of the catalysts. In addition, mapping was conducted to observe the dispersion state of the Ni particles. To estimate the BET surface area of the samples was recorded N2 adsorption isotherms by using a Micromeritics (TriStar-II) instrument.

Electrochemical measurements were performed by using a CHI-660C workstation unit. Pt mesh, Glass carbon electrode, and Ag/AgCl were used as counter electrodes, working electrodes, and reference electrodes, respectively. All measurements were recorded under alkaline conditions at room temperature. The impedance spectrum was performed within the frequency range of 10−1 -105 Hz at constant potential (0.7V). To prepare the catalyst ink, 5 mg of catalyst was dispersed in 100 μL 2-propanol and 5 μL Nafion (was used as a binder agent) solution by ultrasonication for 20 min. Then, 10 μL catalyst ink was dropped onto the GCE and dried at 50 °C.

Results and Discussions

Figures 1a and b illustrate SEM images of powder of Ni and Ni@s-rGO recording with two different magnifications. When looking at the Ni nanoparticles outlook, it was observed that formed like a chain consisting of an oval-like structure. However, after the deposition of Ni on s-rGO, the morphology of particles was changed and their size got smaller. It was concluded that thanks to S-rGO the Ni particles formed with ultra-nanosize and porous structure. Through EDX measurement, it was understood that the catalysts include Ni, C, S, and O elements (Figure 1c). While S belongs to the SDBS, observed O implies that the deoxygenation process was not completed literally. The mapping result exhibits Ni was deposited on the graphene layer homogeneously (Figure 1d).
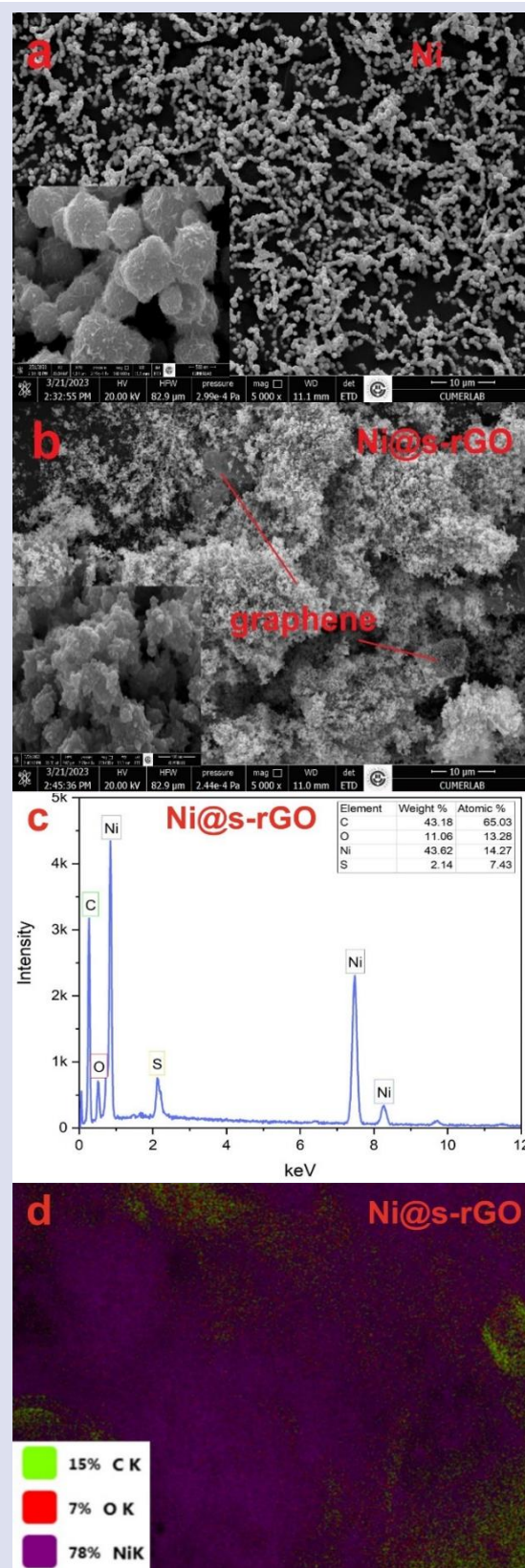

Figure 1. SEM image of a) Ni b) Ni@s-rGO c) EDX spectrum and d) mapping result of Ni@s-rGO

BET analysis

To compare the surface area of samples N_2 adsorption isotherms were recorded as shown in Figure 2. While the quantity adsorbed value for Ni/GCE is 0.4 mmol/g, this value increased to 1.8 mmol/g after being modified with s-rGO. This result exhibits that, the surface area of Ni increased with the contribution of s-rGO.
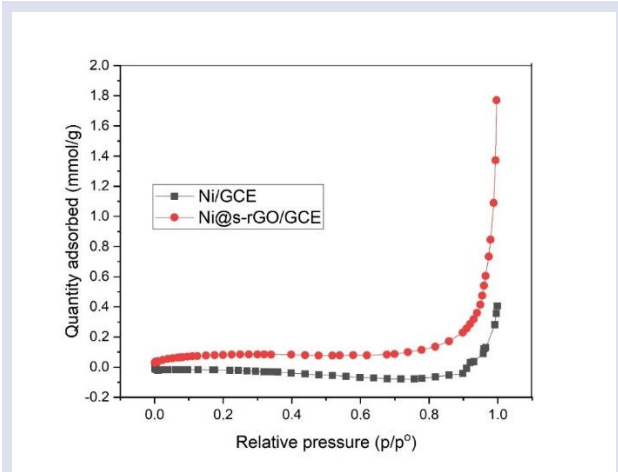

Figure 2. N_2 adsorption isotherm of the Ni/GCE and Ni@s-rGO/GCE

XRD measurement

Figure 3 shows the XRD pattern of Ni/GCE and Ni@s-rGO/GCE in the range of 10° and 90°.In the diffrogram of Ni@s-rGO/GCE, a broader peak was observed at 2θ=22.3° belonging to the S-doped graphene layer. This result is compatible with the earlier study [11].
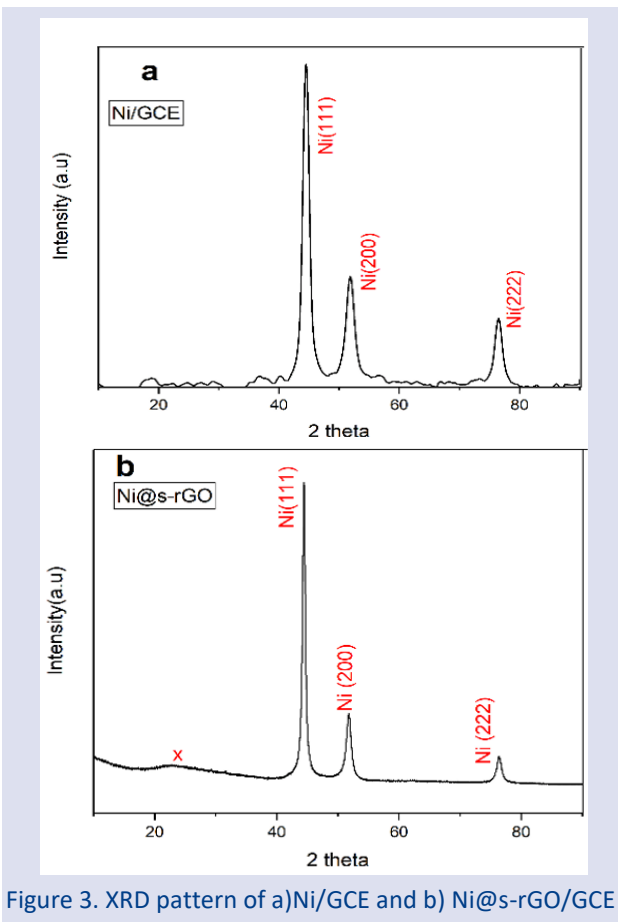

Figure 3. XRD pattern of a)Ni/GCE and b) Ni@s-rGO/GCE

It was concluded that Ni was deposited on both supporting materials with the same crystalline structure is called cubic structure [12]. However, with sharper peak intensity Ni was deposited on s-rGO with a higher density of crystalline form compared to GCE.

The Debye-Scherer equation was used to calculate the average grain size of the samples [13]. From this equation, the average grain size of Ni/GCE and Ni@s-rGO/GCE was calculated as 28 nm and 16 nm, respectively. This result implies that when using s-rGO as a supporting material the particle size of Ni decreased. This result is supported by SEM analysis.

Electrochemical measurement

In Figure 4a before the oxygen evolution peak, a pair of redox peaks was observed around 0.2 and 0.45 V, which is attributed to the $Ni/Ni(OH)_2$ redox couple in Equation [3].

$$Ni + 2OH^- \rightarrow Ni(OH)_2 + 2e^- \qquad (1)$$

$$Ni(OH)_2 + OH^- \leftrightarrow NiOOH + H_2O + e^- \qquad (2)$$
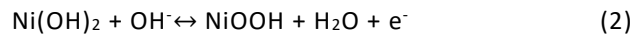
When comparing the peak potential of a pair redox for Ni@GCE and Ni@s-rGO/GCE, the formation of NiOOH on s-rGO occurred at lower potential indicating it needs lower energy.

Figure 4b and 4c show comparing the cyclic voltammograms of Ni/GCE and Ni@S-rGO/GCE with and without MeOH in NaOH. In the presence of methanol, observed a pair of redox peaks disappeared and the current density increased in the anodic region corresponding methanol oxidation. Figure 4d shows that the current density of methanol oxidation of Ni@S-rGO/GCE is higher than Ni/GCE, because of two potential reasons. First, maybe as a result of the synergistic effect between Ni and S formed higher amount of NiOOH that accelerates the decomposed methanol. This conclusion is suggested by Fleischman et al., with the reaction mechanism as follows equations 1 and 2.

The other reason is linked to the adsorption methanol amount which got higher in the presence of S atoms on the graphene layer [14]. In general, recorded CVs for MeOH oxidation reaction include forward peak current and backward current peak belonging to the CO_2 and carbonaceous species (CO_{ad}) which were adsorbed on the catalyst surface, and the adsorbed carbonaceous species were oxidized, respectively [15].

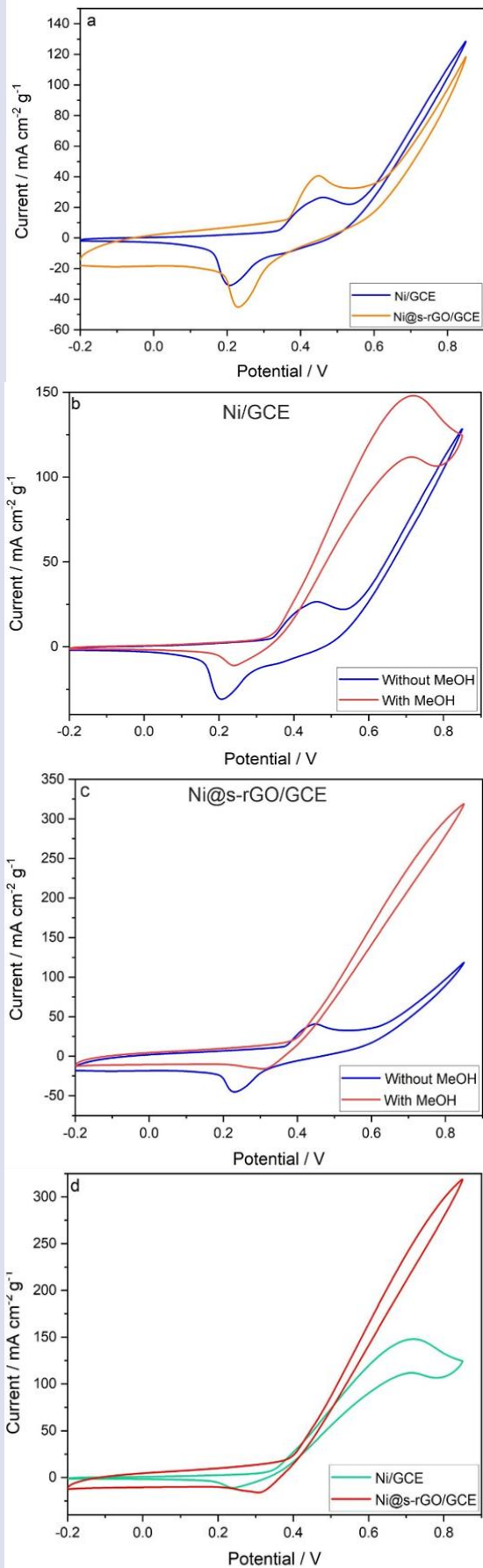$$NiOOH + CH_3OOH(ads) \rightarrow Ni(OH)_2 + CH_2OH + H_2O \qquad (3)$$
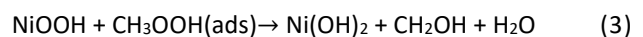
Figure 4. CVs of a) Ni/GCE and Ni@S-rGO/GCE in 0.5 M KOH, b) Ni/GCE, c) Ni@S-rGO/GCE in 0.5 M KOH with and without methanol, and d) Ni/GCE and Ni@S-rGO/GCE in 0.5 M KOH including 0.5 M MeOH.

When looking at the anodic region of CVs for both electrodes, only Ni@GCE CVs include backward peak current. From these observations, it was concluded that poisoning species such as CO, and COOH don't adsorb on Ni@S-rGO/GCE. Therefore it can be said, it has good anti-poisoning properties.

Figure 5a illustrates the cyclic voltammograms of methanol oxidation on the Ni@S-rGO/GCE for different methanol concentrations ranging from 0.1 to 1 M. It was observed that current density increased gradually with methanol concentrations. However, when the concentration reached 1M, the current became constant indicating that the active sites of the electrode were saturated with methanol.
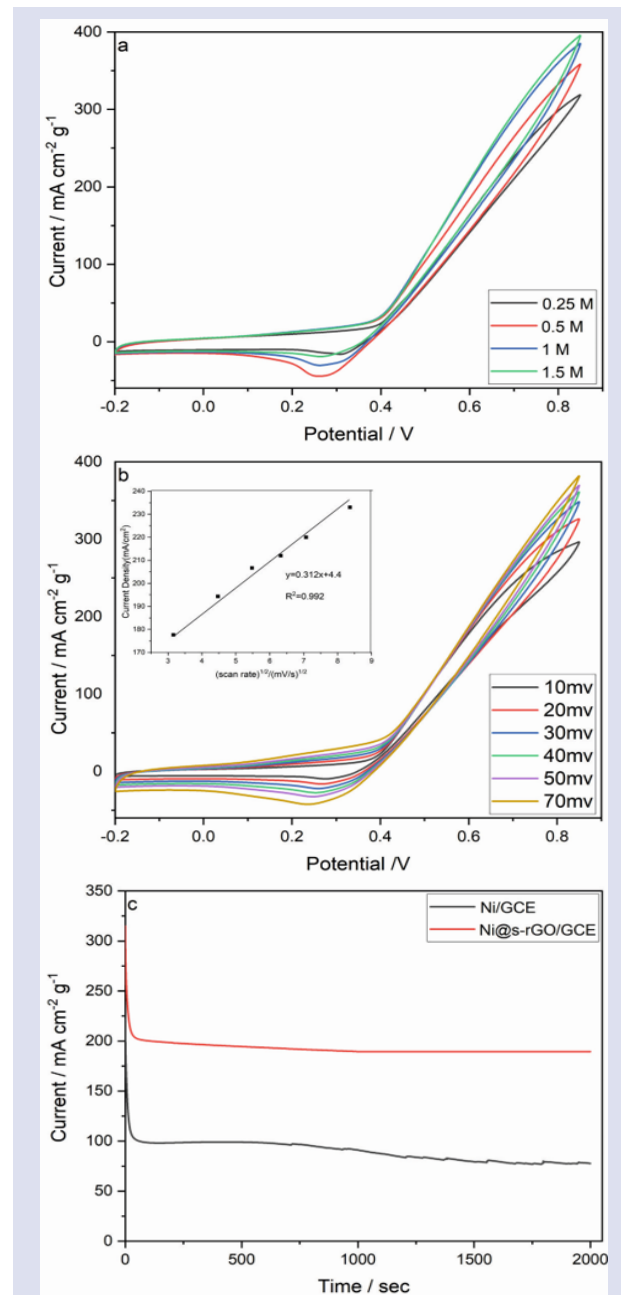

Figure 5. CVs of Ni@s-rGO/GCE a) in 0.5 M KOH including variation concentration of methanol b) at different scan rates in 0.5 M KOH including 0.5 M MeOH c) amperometric measurement of Ni@GCE and Ni@s-rGO/GCE at a constant potential.

The catalytic kinetics of Ni@S-rGO/GCE for the methanol electrooxidation reaction was studied at various scan rates from 10 to 70 mV/s in the presence of 0.5 M methanol in 0.5 M KOH solution. The current density of methanol oxidation increases with the scan rate as shown in Figure 5b. The Inset figure in Figure 5b shows a plot of peak current density versus the square root of the scan rate ($v^{1/2}$). The linear response of the graph shows that the reaction occurred under diffusion-controlled conditions [15].

Figure 5c shows the chronoamperometric measurement of Ni@GCE and Ni@s-rGO/GCE for methanol oxidation in KOH including 0.5 M methanol. Due to the anti-poisoning property and decomposition capability of methanol Ni@s-rGO/GCE exhibits higher current intensity when compared to Ni@GCE. Besides, the current density value of Ni@s-rGO/GCE remains with time. Therefore, from these results, it was concluded that Ni@s-rGO/GCE shows higher stability and good anti-positioning properties for methanol oxidation.

Electrochemical impedance spectroscopy measurement

Two semicircles are observed in the Nyquist diagrams of Ni@GCE and Ni@S-rGO/GCE in Figure 6. While the semicircle diameter in the high-frequency region is associated with the electrical conductivity of the electrode, the semicircle diameter in the low frequency is related to the resistance of charge mobility [16]. From Table 1, Ni@S-rGO/GCE has higher conductivity and charge mobility compared to Ni@GCE. When looking at the CPE1-T values of both electrodes in Table 1, the CPE-T value of Ni@S-rGO/GCE is three times higher than Ni@GCE, associated with depositing the higher amount of methanol on Ni@S-rGO/GCE. From EIS measurement, it was concluded that the catalytic activity of Ni@S-rGO/GCE was higher than Ni@GCE for MOR because it provides active sites for adsorption methanol and enhances charge mobility so the reaction rate.
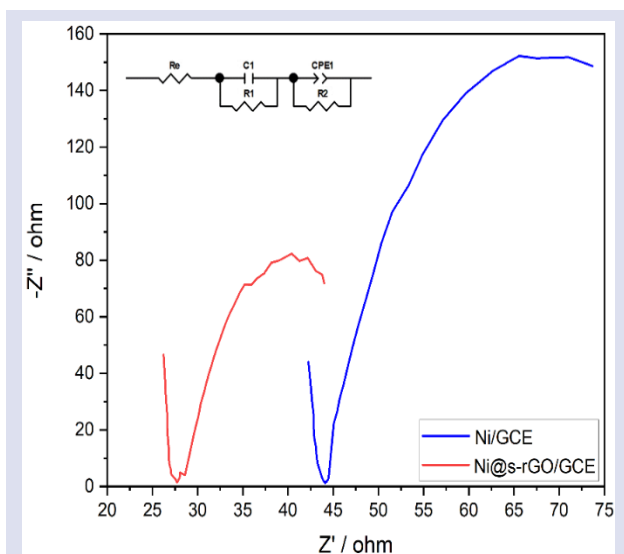

Figure 6. Nyquist diagram of Ni@GCE and Ni@s-rGO/GCE (inset: equivalent circuit for both electrode

Table 1. Fitting result of EIS measurement of Ni@GCE and Ni@s-rGO/GCE

Electrode	C1(nF)	R1 (Ω)	CPE1-T	CPE1-P	R2 (Ω)
Ni@GCE	5.1	42.68	0.002	0.78	46.4
Ni@S-rGO/GCE	4.73	26	0.006	0.46	29.83

Conclusion

We have presented a facile method for synthesizing Ni with ultra nano-size particles which promote the oxidation of methanol. Ni was fabricated on S-doped reduced graphene oxide. The graphene layer acted as a supporting material for the deposition of Ni homogenously and thanks to S atoms Ni particles formed with smaller size. Due to the synergistic effect between Ni and S, the oxophilitcy of Ni enhanced so the number of Nickel oxyhydroxides which are the active sites for methanol oxidation increased. Therefore, comparing the catalytic activity of Ni@rGO and Ni@s-rGO has two times higher mass activity which implies increased the methanol oxidation reaction rate. From the amperometric measurement, it was concluded that after the deposition of Ni on s-rGO, the obtained catalyst became stable against poisoning types. To sum up, with S-doped reduced graphene oxide, Ni nanoparticles show excellent catalytic activity towards methanol oxidation.

Conflicts of interest

There are no conflicts of interest in this work.

References

[1] Mei J., Hou G., Zhang H., Chen Q., Cao H., Tang Y., Zhang J., Zheng G., Convenient construction of porous dendritic Cu-doped Ni@PPy/stainless steel mesh electrode for oxidation of methanol and urea, *Applied Surface Science*, 623 (2023) 156930.

[2] Mahapatra S.S., Datta J., Characterization of Pt-Pd/C Electrocatalyst for Methanol Oxidation in Alkaline Medium, *International Journal of Electrochemistry*, (2011) 563495.

[3] Wu D., Albert M., Soldan A., Pettigrew C., Oishi K., Tomogane Y., Ye C., Ma T., Miller M.I., Mori S., Multi-atlas based detection and localization (MADL) for location-dependent quantification of white matter hyperintensities, *NeuroImage: Clinical*, 22 (2019) 101772.

[4] Liu C., Yang F., Schechter A., Feng L., Recent progress of Ni-based catalysts for methanol electrooxidation reaction in alkaline media, *Advanced Sensor and Energy Materials*, 2 (2023) 100055.

[5] Samimi G., Ashrafi H., Tashkhourian J., Haghighi B., rGO@Ni/NiO composite an effective electrocatalyst for methanol oxidation reaction in alkaline media, *Journal of Physics and Chemistry of Solids*, 184 (2024) 111724.

[6] Wang J., Zhao Q., Hou H., Wu Y., Yu W., Ji X., Shao L. Nickel nanoparticles supported on nitrogen-doped honeycomb-like carbon frameworks for effective methanol oxidation, *RSC Advances*, 7 (2017) 14152–14158.

[7] Sun H., Ye Y., Liu J., Tian Z., Cai Y., Li P., Liang C., Pure Ni nanocrystallines anchored on rGO present ultrahigh electrocatalytic activity and stability in methanol oxidation, *The Royal Society of Chemistry*, 54 (2018) 1563-1566.

[8] Raluca Tarcan R., Todor-Boer O., Petrovai I., Leordean C., Astilean S., Botiz I., Reduced graphene oxide today, *The Royal Society of Chemistry*, 8 (2020) 1198-1224.

[9] Sundaram R.S., Chemically derived graphene, Graphene. *Cambridge: Elsevier*, (2014) 50-80.

[10] Hummers W.S., Offeman R.E., Preparation of Graphitic Oxide, . *Am. Chem. Soc*, 80 (1958) 1339.

[11] Kaplan S., Suna Karatekin R., Kahya Dudukcu M., Avcı G., A novel Ni-Fe$_3$O$_4$@s-rGO/GCE electrode for electrochemical detection of H$_2$O$_2$, *Materials Chemistry and Physics*, 294 (2023) 127051.

[12] Taghizadeh F., The study of structural and magnetic properties of NiO nanoparticles, *Optics and Photonics Journal*, 6 (2016) 164-169.

[13] Kumar P R., Prasad N., Veillon F., Prellier W., Raman spectroscopic and magnetic properties of Europium doped nickel oxide nanoparticles prepared by microwave-assisted hydrothermal method, *Journal of Alloys and Compounds*, 858 (2021) 157639.

[14] Suna Karatekin R., Kaya D., Kaplan S., Kahya Düdükcü M., Effect of the configurations of N and S atoms on electrochemical performance of Pt for methanol oxidation, *Journal of Nanoparticle Research*, 24 (2022) 233.

[15] Suna Karatekin R., Kaplan S., Ildan Ozmen S., Kahya Düdükcü M., Enhanced methanol oxidation on N-doped reduced graphene oxide/ZnO/nano-Pt catalyst, *Diamond & Related Materials*, 127 (2022) 109145.

[16] Karazehir T., Electrodeposited Pd nanoparticles on polypyrole/nickel foam for efficient methanol oxidation, International *Journal of Hydrogen Energy*, 48 (2023) 10493-10506.